Supporting Information for

Photophysical Pore Control in an Azobenzene-Containing Metal-Organic Framework

Jonathan W. Brown, [†,*,°] *Bryana L. Henderson,* [§,°] *Matthew D. Kiesz,* [§] *Adam C. Whalley,* [‡] *William Morris,* [†] *Sergio Grunder,* [‡] *Hexiang Deng,* [†] *Hiroyasu Furukawa,* [†] *Jeffrey I. Zink,* [§] *J. Fraser Stoddart,* [‡] *Omar M. Yaghi* [†,v,*].

[†] Center for Reticular Chemistry, Center for Global Mentoring, and Department of Chemistry and Biochemistry, University of California, Los Angeles, California 90095, United States

[§] Department of Chemistry and Biochemistry, University of California, Los Angeles, 607 Charles E. Young Drive East, Los Angeles, California 90095-1569, United States

[‡] Center for the Chemistry of Integrated Systems and Department of Chemistry, Northwestern University, 2145 Sheridan Road, Evanston, Illinois 60208, United States

[v] Department of Chemistry, University of California, Berkeley, California, 94720, United States

Molecular Foundry, Division of Materials Sciences, Lawrence Berkeley National Laboratory,

Berkeley, California, 94720, United States

NanoCentury KAIST Institute and Graduate School of EEWS (WCU), Korea

Section S1: Materials and general procedures

All reagents unless otherwise stated were obtained from commercial sources (Cambridge isotope laboratories, Sigma Aldrich, TCI) and were used without further purification. Yields reported were unoptimized.

Section S2: Synthesis of azo-IRMOF-74-III

IRMOF-74-III azo [$Mg_2(C_{26}H_{16}O_6N_2)$] was synthesized by combining $Mg(NO_3)_2 \cdot 6H_2O$ (80 mg, 0.315 mmol) and the azobenzene-functionalized linker (42.5 mg, 0.09 mmol) in a solution of N,N-dimethylformamide (DMF) (7.5 mL), EtOH (0.5 mL) and H_2O (0.5 mL) for 24 h at 120 ˚C. After 24 h, the red crystals were collected by filtration. The crystals were washed with DMF (3 x 10 mL) over a thirty-minute period. The DMF was then replaced with MeOH (6 x 30 mL) over a two-day period. Finally, the volatile MeOH was removed by using a supercritical CO_2 dryer. The crystals were then heated at 250 ˚C under vacuum (30 mtorr) for 12 hrs.

Section S3: Structure resolution of azo-IRMOF-74-III from Powder X-Ray Diffractrometry (PXRD)

Powder X-ray data were collected using a Bruker D8-Discover θ-2θ diffractometer in reflectance Bragg-Brentano geometry employing Ni filtered Cu Kα line focused radiation at 1600 W (40 kV, 40 mA) power and equipped with a Vantec Line detector. Radiation was focused using parallel focusing Gobel mirrors. The system was also outfitted with an anti-scattering shield that prevents incident diffuse radiation from hitting the detector, preventing the normally large background at $2\theta < 3$. Samples were mounted on zero background sample holders by dropping powders from a wide-blade spatula and then leveling the sample with a razor blade. To determine the structure of IRMOF-74-III azo, crystal structure modeling was carried out, followed by Rietveld refinement.

Crystal structure modeling. The model for IRMOF-74-III azo, including cell parameters and atomic positions, was generated using Materials Studio chemical structure-modeling software[i] employing the Crystal Building module. The structure was generated using the relevant space group, the cell parameters were used as obtained, and atom positions were generated from the refined data of extended MOF-74.[ii] The constructed structure was minimized with the Forcite module using the Geometry Optimization routine with the Universal force field (UFF).[ii] The obtained model was used as input for the Rietveld refinement. Positions of atoms in the respective unit cells are listed as fractional coordinates in Table S1.

Table S1: Fractional atomic coordinates for azo-IRMOF-74-III calculated from the *Materials Studio software.*

Azo-IRMOF-74-III				
Space Group R 3 *a* = *b*= 46.771(46)Å *c* = 6.869(83)Å α = β = 90˚ γ = 120˚		Volume 15028 Å^3		
Atom	**Occupancy**	**X**	**Y**	**Z**
H1	1	0.30123	0.14934	0.54529
H2	1	0.30397	0.19166	0.31701
H3	1	0.69359	0.87253	0.42753
H4	1	0.69335	0.91513	0.21653
H5	1	0.66974	0.91562	0.92056
H6	1	-0.01108	0.26389	0.56726
H7	1	0.66141	0.0613	1.02123
H8	1	0.01907	0.42756	0.66852
H9	1	0.99434	0.43105	0.36945
H10	1	0.99896	0.47534	1.15234
H11	1	0.38835	0.15284	1.26852
C1	1	0.32144	0.15974	0.43725
C2	1	0.32324	0.18422	0.30619
C3	1	0.68211	0.86497	0.82752
C4	1	0.6874	0.91552	0.36921

C5	1	0.68854	0.89138	0.49187
C6	1	0.68279	0.89141	0.6933
C7	1	0.67539	0.91589	0.76748
C8	1	0.93122	0.27557	0.61028
C9	1	0.93085	0.26837	0.81376
C10	1	0.95774	0.28938	0.94348
C11	1	0.70221	0.04823	0.6461
C12	1	0.72712	0.07259	0.77487
C13	1	0.72793	0.06653	0.97879
C14	1	0.01307	0.4278	0.82095
C15	1	1.00889	0.45444	0.89296
C16	1	1.00236	0.45509	1.09247
C17	1	1.0002	0.42969	0.21749
C18	1	1.01146	0.48142	0.75876
C19	1	0.37001	0.16151	0.28003
C20	1	0.37251	0.1865	1.14965
O1	1	0.98797	0.26319	0.42254
O2	1	0.95415	0.30335	0.5335
O3	1	0.98405	0.3162	0.88166
O4	1	0.95565	0.28113	1.12396
O5	1	0.70233	0.05569	0.4655
O6	1	0.67974	0.01894	0.70892
O7	1	0.70922	0.03722	1.05563
O8	1	0.66102	0.06141	0.16604
Mg1	1	0.98848	0.30608	0.34006
Mg2	1	0.6723	0.02583	0.25001
N	1	0.46947	0.53429	1.33391
N	1	0.43939	0.52951	1.30546
C	1	0.43532	0.54818	0.14561
C	1	0.46125	0.56422	0.00442
C	1	0.45837	0.58349	-0.14622
C	1	0.42951	0.58708	-0.15782
C	1	0.40365	0.57154	-0.01833
C	1	0.40662	0.55238	0.1328

Section S5: Comparison of Propidium Iodide to azo-IRMOF-74-III aperture

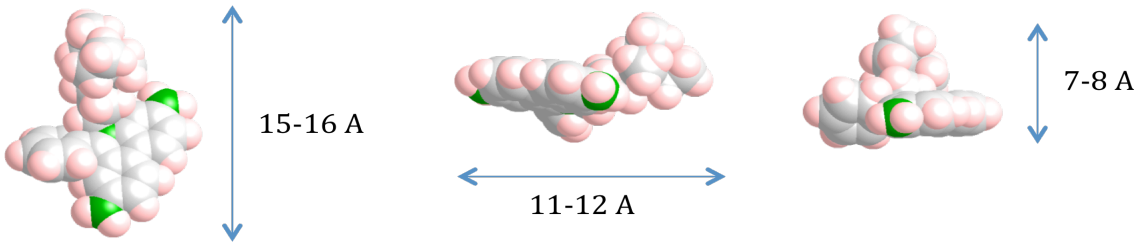

Figure S-1: Propidium Iodide size without counterion in three dimensions

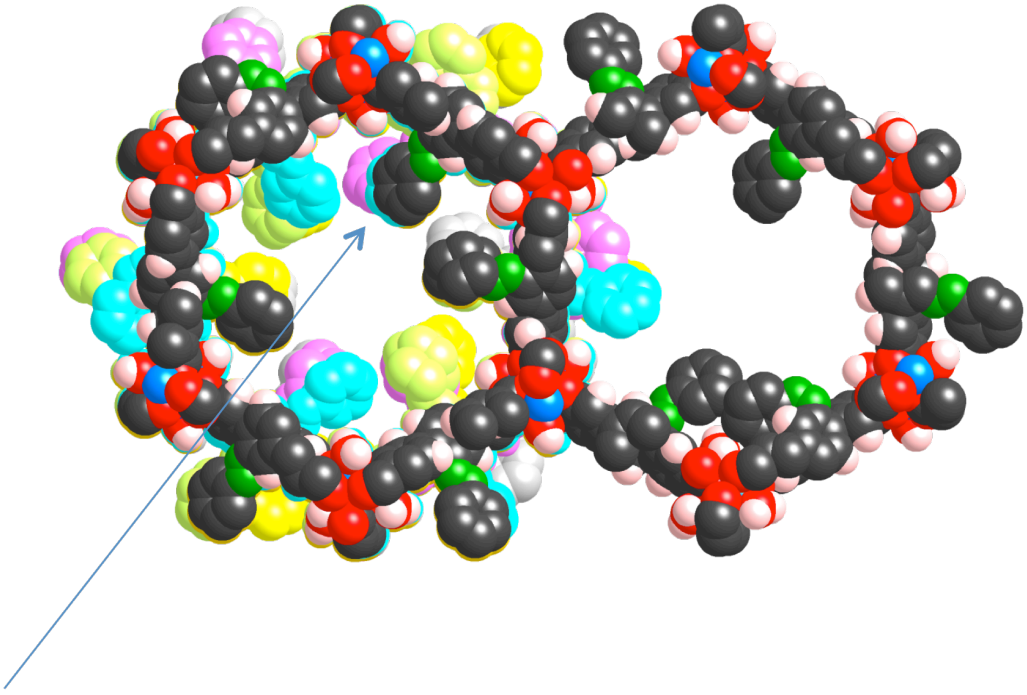

Figure S-2: Space filling model of non-idealized azo-IRMOF-74-III

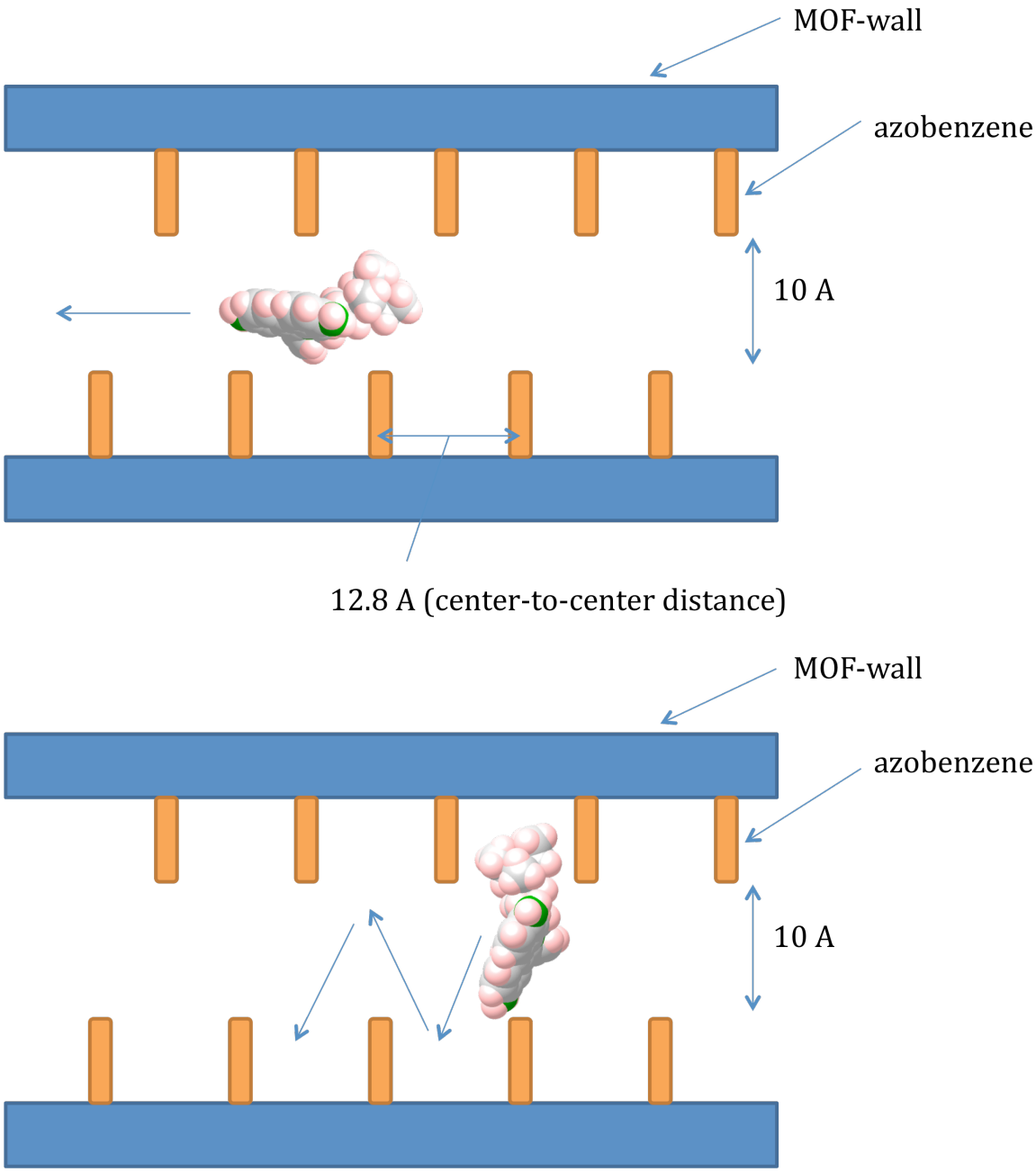

Figure S-3: Comparison of dye diffusion with different orientation through MOF structure

While it may be possible for a dye which is oriented perfectly perpendicular to the pore channels to escape in dark conditions, other orientations may cause blockage and dye diffusion is limited. Additionally, interactions with the pore wall and collisions with solvent and counter ions hinder motion through the pore. With photoswitching of the azo-species from trans to cis, mobility is enhanced.

Section S5: Thermal gravimetric analysis of azo-IRMOF-74-III

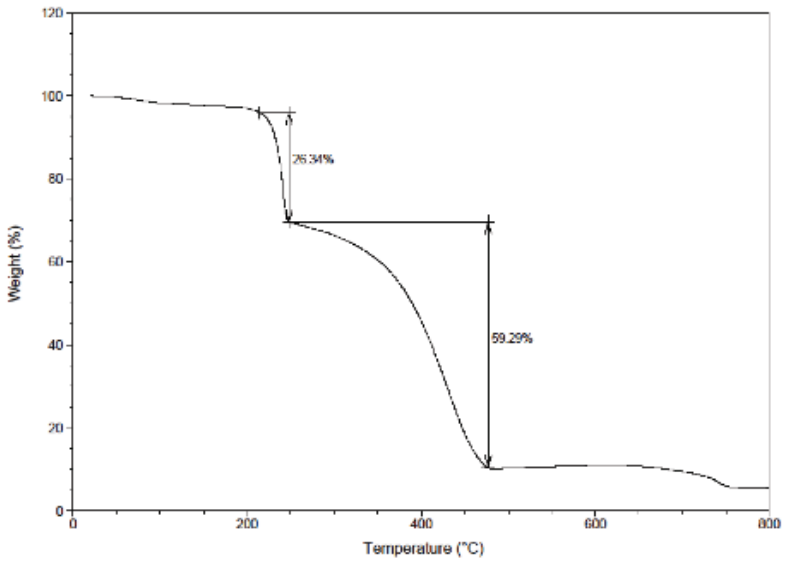

Figure S-4: Thermal gravimetric analysis of azo-IRMOF-74-III while heating sample from 20-800°C

Section S6: Solid-state ^{13}C CP/MAS nuclear magnetic resonance spectroscopy.

High Resolution solid-state nuclear magnetic resonance (NMR) spectra were recorded at ambient pressure on a Bruker DSX-300 spectrometer using a standard Bruker magic angle-spinning (MAS) probe with 4 mm (outside diameter) zirconia rotors. The magic angle was adjusted by maximizing the number and amplitudes of the signals of the rotational echoes observed in the ^{79}Br MAS FID signal from KBr.

Cross-polarization with MAS (CP/MAS) was used to acquire ^{13}C data at 75.47 MHz. The ^{1}H and ^{13}C ninety-degree pulse widths were both 4 ms. The CP contact time varied from 1.5 to 5 ms. High power two-pulse phase modulation (TPPM) ^{1}H decoupling was applied during data acquisition. The decoupling frequency corresponded to 72 kHz. The MAS sample-spinning rate was 10 kHz. Recycle delays between scans varied between 3 and 10 s, depending upon the compound as determined by observing no apparent loss in the ^{13}C

signal from one scan to the next. The ^{13}C chemical shifts are given relative to tetramethylsilane as zero ppm, calibrated using the methylene carbon signal of adamantane assigned to 37.77 ppm as the secondary reference.

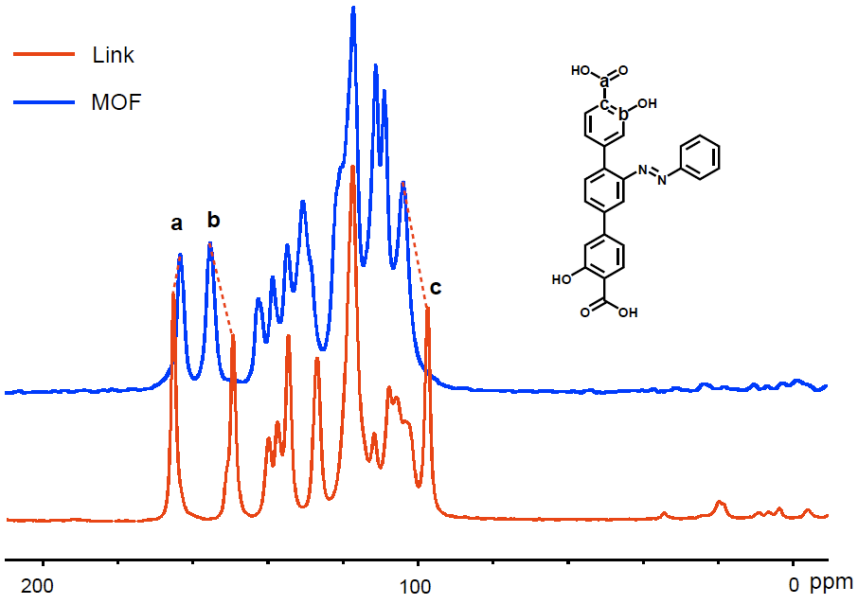

Figure S-5: ^{13}C NMR of azobenzene link and azo-IRMOF-74-III in the solid state.

Section S7: Fluorescence monitoring of wavelength specific release experiment

The fluorescence of the solvent above a 100 mg sample of azo-IRMOF-74-III loaded with propidium iodide was monitored with a 448 nm laser in a setup identical to the other release studies within this paper. After a baseline was established, a 647 nm laser was focused on the sample of particles; no release was observed. Subsequently, a 403 nm laser was focused on the sample and an immediate increase in the fluorescence signal was observed.

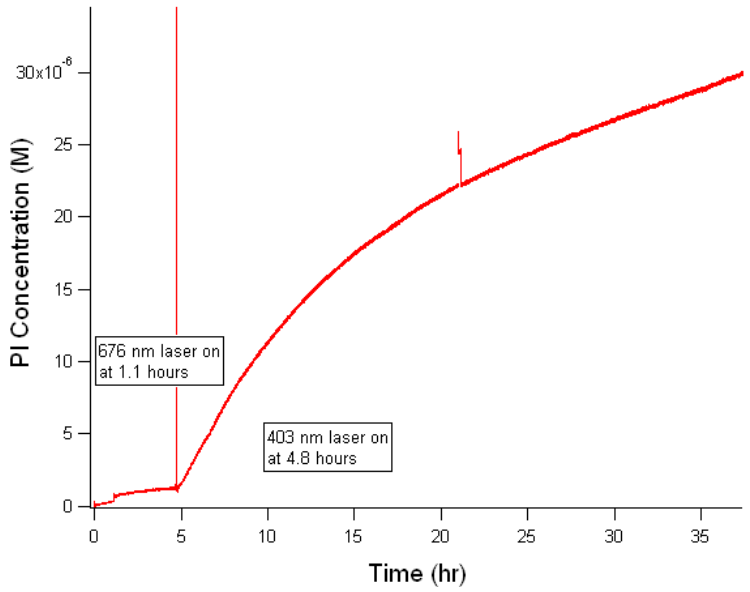

Figure S-6: Time-dependent concentration of propidium iodide released from azo-IRMOF-74-III under sequential exposure to 647 nm and 403 nm lasers.

Section S8: UV-vis determination of loading efficiency of propidium iodide into azo-IRMOF-74-III

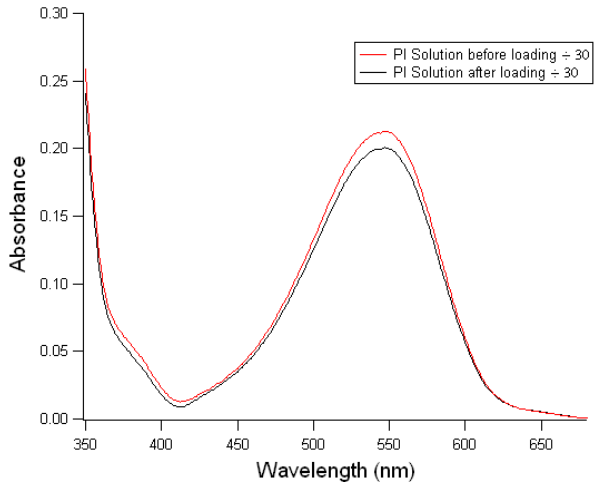

Figure S-7: UV-vis spectra of a propidium iodide solution before and after loading a 100 mg sample of azo-IRMOF-74-III for three days. The 6% difference in concentration corresponds to the amount of dye uptaken by the particles.

Section S9: UV-vis spectra of an ethanol solution of the azo-linker and magnesium chloride

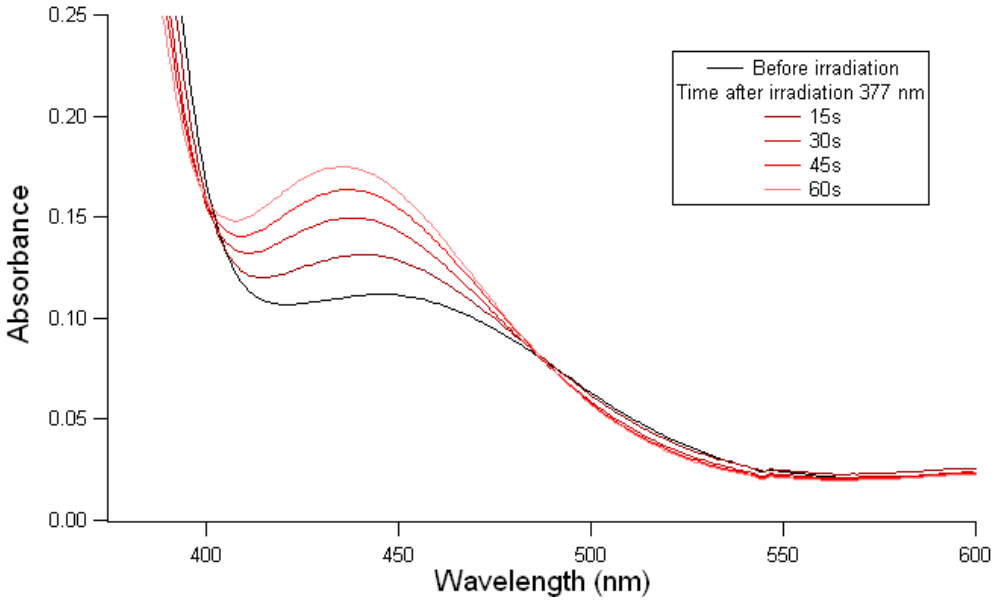

Figure S-8: Absorption spectra of a 0.2 mM azo-linker and 0.8 mM $MgCl_2$ solution in ethanol before and after exposure to 377 nm light for 15 s intervals. An isosbestic point at 403 nm is observed.

---

[i] Materials studio version 5.0, 2009, Accelrys Software Inc.

[ii] H. Deng, S. Grunder, K. E. Cordova, C. Valente, H. Furukawa, M Hmadeh, F. Gandara, A. C. Whalley, Z. Liu, S. Asahina, H. Kazumori, M. O'Keeffe, O. Terasaki, J. F. Stoddart, O. M. Yaghi, *Science*, **2012**, *336*, 6084, 1018-1023.